

Research Article

The Effects of Pore Size and Percentage Composition of Air Voids on Impact Energy Absorption of Al Foam using Numerical approach

Seyfu Tiruneh Debebe

Addis Ababa University, Addis Ababa institute of Technology, School of Mechanical and Industrial Engineering, Addis Ababa, Ethiopia.

Received: 12 December 2022

Revised: 19 January 2023

Accepted: 02 February 2023

Published: 13 February 2023

Abstract - Recently, there has been a high interest in using lightweight aluminum foams for automotive, railway and aerospace operations. Because of its high ductility and deformability, Aluminum foam is generally used for energy absorption for crashworthiness applications. To keep safe and avoid occupant injuries, it is necessary to absorb the kinetic energy generated during impact. Thus, to absorb high kinetic energy, the crash box material needs a special material microstructure, which is light in weight and can absorb further energy than the being one like $CaCo_3$, CBC, or SiC. B4C etc. In particular, the analysis of energy absorption of aluminum foam in automotive for energy absorption applications is limited. The main objective of this exploration is to analyze and optimize the porosity size and voids percentage on impact energy absorption of aluminum foam using a numerical approach. For this purpose, first, fifteen CAD Al foam samples were developed by using Digimat multi-scale material modeling software. Second, cubic elements with circular bubble shape at 5, 10 and 15 void percentage and at 1.5 mm, 2 mm, 2.5 mm, 3 mm and 3.5 mm bubble sizes were modeled. Finally, the numerical analysis of impact energy by using ANSYS workbench19.2 Explicit dynamics by applying initial low velocity was performed. The parameters were compared to each other to optimize the proper percentage composition and cell size for the best energy absorption applications. The effects of bubble shape, foaming agent and percentage composition on energy immersion were discussed. In this study, the analysis was fulfilled by determining and comparing the energy absorptions of all the models and, finally, comparing them with existing foaming agents.

Keywords - Absorption energy, Aluminum foam, Digimat, Fem analysis, Impact, Voids.

Nomenclature

R	Radius	M	Thermal softening constant
nRi	n-Void fraction and i-bubble size	m	mass
A	Initial yield stress	MF	Mean Field
Al	Aluminum	MPa	Mega pascal
B	Hardening constant	N	Number of cells
C	Strain rate constant	n	Hardening exponent
V	Volume	R	Radius
CD	Cell density	ϵ^{pl}	Equivalent plastic strain
COR	Coefficient of restitution	$\epsilon^{(*pl)}$	Equivalent plastic strain rate
E	Energy	ρ^{*}	Relative density
FE	Finite Element	ρ^f	Density of the foam
SEA	Specific Energy Absorption		
P	Porosity		

1. Introduction

Metal foams are a new class of materials of great interest due to their unique combination of parcels deduced from their cellular structures and metallic geste as well as a seductive material for factors of the vehicle in automotive diligence for rudiments absorbing impact energy, adding

stiffness and improving the passenger safety by reducing vibration, noise and due to their high strength to weight rate.

They are excellent impact energy absorbers, and they can convert impact energy into deformation energy and absorb further energy than bulk essence during contraction (1). In particular, aluminum foams demonstrate a number of interesting parcels due to their featherlight and pervious



structure, making them usable in a wide range of operations in automotive diligence. To enhance the performance of aluminum foam, fine ceramics complements similar to cubic boron nitride (CBN), silicon carbide (SiC), and boron carbide (B4C) can be incorporated into aluminum foams to their performances. LI et al. (2) investigated the mechanical parcels and the energy immersion capability of the corroborated aluminum foam under dynamic and quasi-static contraction loading conditions. Their result shows that the addition of CBN-modified aluminum foam displayed the loftiest energy capability under dynamic and quasi-static contraction tests as compared to the independent SiC and B4C modified aluminum foams. According to a British Vehicle Insurance Repair Research Center study on vehicle impact damage occurs, 65 were frontal impacts, 25 were hinder impacts, and 10-sided impacts(2). Thus, the crash box dissipates crash energy using an energy-absorbing foamed specimen.

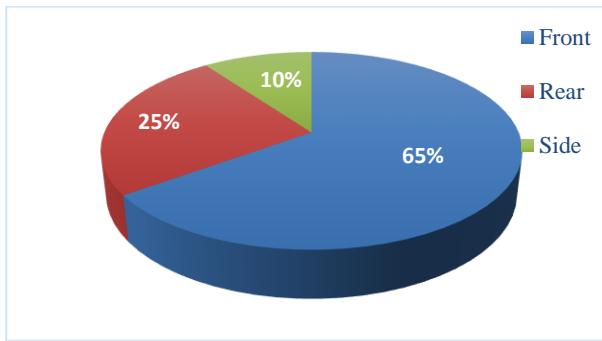


Fig. 1 Crash statistics [2]

Fig. 2 shows the physical structure of the crash box for automotive applications.

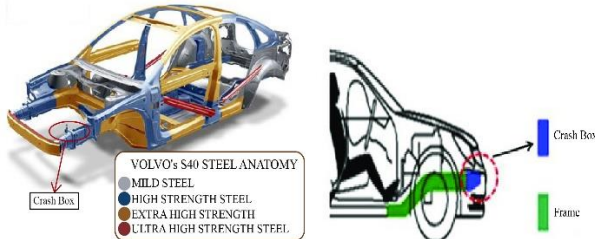


Fig. 2 Physical structure of the crash box for vehicle application [3][4]

As the above figure shows, the crash box structure is assembled in front of the car between the bumper beam and the front car cabin/structure. As Figure 1 shows, frontal impacts are the first and ultimate severe car accident crashes. In the case of a vehicle crash, the occupant's safety is of prime concern, and this demands that the vehicle form be designed to withstand high-impact forces [5]. In the case of impact/crash, the requirement is achieved through a properly designed high-energy incorporation system. For these

structures, Aluminum foams have the potential to absorb impact strength during the crashing of a vehicle, either against another vehicle or a pedestrian. To protect the occupants of a car, various safety features, such as airbags, crash boxes, and seat belts, were used for crash box constructions. Among those, crash boxes are a separate structure in a vehicle that is mounted between the car's mainframe and front bumper. The crash box structure is expected to collapse and absorb crash energy before the other body parts so that damage in the main cabin frame is minimized and passengers are saved their lives. The problems identified to conduct the study are the loss of passenger life by car crash accidents (51% up to 65% by a frontal crash), the damage of expensive car components behind the crash box and limitations of daily investigations on absorbent Al foam materials for crash box utilizations.

It has been established that the strength and energy absorption features of closed-cell aluminum alloy foam possibly improved through tailored microstructure designs. To keep safe and prevent occupant injuries, it is necessary to absorb the kinetic energy generated during a head-on collision. Therefore, to absorb high kinetic energy, the crash box material needs a special material microstructure improvement, which is good energy absorbing capacity and is lightweight to save fuel economy. On the other hand, the distribution of filler and foaming agents for the foam microstructure greatly plays an important role in the energy absorption of Al foam. Strengthening a structure is to dissipate the crash energy to prevent injuries and improve the crashworthiness of the structure; an optimum combination of the material's microstructure (bubble distribution, bubble size and porosity percentage) throughout the entire model are needed. Therefore, in addition to all investigations on Al foam, it is necessary to analyze energy absorber specimen from lightweight closed-cell aluminum foam capable of absorbing high-impact energy. Generally, this paper focuses on evaluating and optimize the effects of pore size, foaming agent and voids percentage composition on the energy absorption of Aluminum foam using the numerical approach.

1.1. Aluminum Foam

Aluminum foam is a porous metallic material created by adding a foaming agent in the way that air for bubbling molten aluminum during production. The density of Al foam varies from 0.2 to 0.4 g/cm³ [7], less than 94.8% and 85.2% density of steel and solid Al, respectively. Because of its specific strength and high resistance under compressive loading, it is suitable for lightweight structures and the absorption of impact energy. the capability of absorbing the impact energy during a car crash is one of the ultimate interesting properties of aluminum foams.

2. Methodology

The general summarized methodology used for this paper is shown in

below.

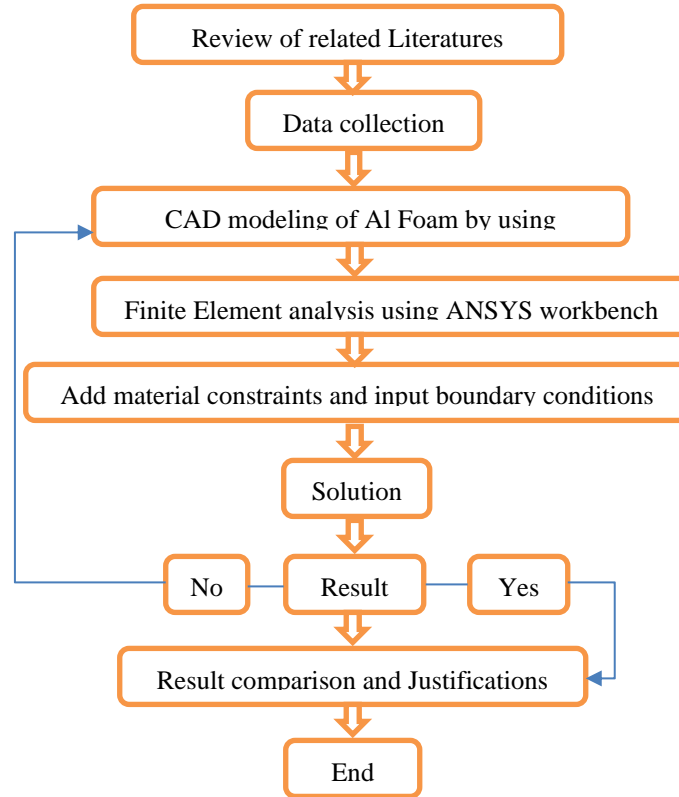


Fig. 3 Summarized methodology for the study

1.2. Description of FEA Methods

The DIGMAT multi-scale material modeling is used to develop the CAD Al foam with uniform cell diameter and randomly distribute the voids inside the cubic element.

Explicit dynamic simulations are best performed on prismatic rectangular and cubic specimens of foam with a specimen dimension at least seven times greater than the unit cell of pore or air void size according to the ASTM standard. In modeling the specimen, the minimum dimension of the specimen is greater than seven times the pore size. This avoids the porosity size effect[8][9]. In impact simulation, decreasing and increasing the number of bubble cells leads to analyzing, evaluating and characterizing the foam's mechanical properties.

1.2.1. Material properties of Aluminum 7075-T6 Alloy

This category of aluminum alloy is typically found in automotive, aviation, marine and other transport applications because of its extremely high ratio of strength to density[10]. Aluminum foam developed

from Al 7075-T6 alloy is the best material for blast and impact energy absorption applications because of the following mechanical properties.

Table 1. Physical and mechanical properties of Al7075-T6.

Properties	Values
Density (kg/m ³)	2800
Poisson's ratio	0.33
Elastic modulus (GPa)	71.7
Yield strength (MPa)	503
Elongation (%)	11
Hardness (HB500)	87
Shear strength (MPa)	331

3. Material Modeling

Johnson Cook plasticity model is used for impact numerical modeling of the Al foam using finite element ANSYS. The Johnson-Cook plasticity model (Equation 1) describes the dependency of plastic flow stress (σ) on equivalent plastic strain (ϵ^{pl}), equivalent plastic strain rate ($\dot{\epsilon}^{*pl}$) and temperature (T)[11]. The material model for the Al 7075-T6 is modeled by means of the Johnson-Cook material model contained in the FEA ANSYS code.

$$\sigma = [A + B(\epsilon_{pl})^n] [1 + C \ln(\dot{\epsilon}^{pl} / \dot{\epsilon}^{*pl})] (1 - T^*) \dots\dots\dots 1$$

Where the first term represents the strain hardening of the yield stress, the second term indicates the increase in the yield stress at elevated strain rates, and the final term represents the decrease in the yield stress due to local thermal effects. A, B, C, n and m are constants. ($\dot{\epsilon}^{pl} / \dot{\epsilon}^{*pl}$) is the normalized equivalent plastic strain rate.

$$T^* = (T - T_{ref}) / (T_{melt} - T_{ref}) \dots\dots\dots 2$$

Where T^* is the temperature, T_{melt} is the melting temperature of the material, and T_{ref} is the reference temperature.

Table 2. J-C material model parameters for Al Alloy 7075-T6[12]

Constants	A(MPa)	B (MPa)	N	c	m
AA7075-T6	546	678	0.71	0.024	1.56

4. CAD Modeling and Finite Element Analysis

4.1. CAD Geometry Modeling Process

Digmat-FE is a micromechanical material modeling software that generates a representative volume element(RVE) of the cubic aluminum foam microstructure at different percentages of porosity. A total of fifteen CADs is developed using Digimat multi-scale material modeling. Those are fifteen cubic boxes with circular bubble (cell) shape at cell radius of (1.5, 2, 2.5, 3 and 3.5) mm with 5%, 10% and 15% volume void fraction. According to [13][14], recommended pore sizes for aluminum foam elements for energy absorption purposes in different application areas and at the industrial level are between 1.5 mm to 3.5 mm[15][16]. For example, in the ALPORAS aluminum foam investigation, an average cell size of 3.5 mm was used[17].

The 3D Voronoi technique generates closed-cell aluminum foam with randomly distributed cells and uniform cell diameters. The 3D Voronoi model is constructed using Digimat multi-scale material modeling software. To minimize possible boundary and size effects (Gibson and Ashby, 1997), the length of the cubic Voronoi foam is set at 30 x 30 x 30 mm for a cubic model with a circular unit cell [18]. It is shown in Figure 5 below.

The number of cells (N) in a Voronoi foam can be calculated by

$$N = V / ((4\pi/3) r^3) \dots\dots\dots 3$$

Where V- is the volume of the cubic box, which is equal to 27,000 mm³.

r- Radius of the cell or bubble, ranging from 1.5 mm – 3.5 mm.

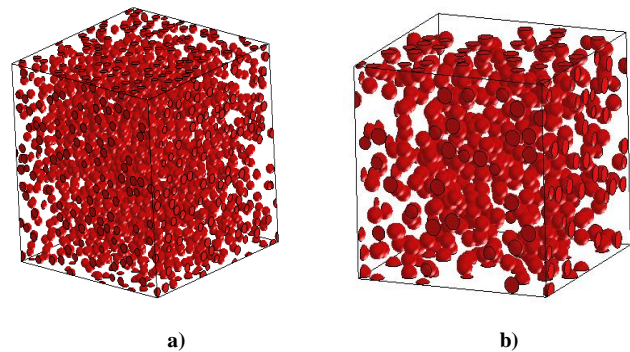
Table 2. Number of bubbles with respective radius

For the entire analysis, five different radius values are used. Now, the number of cells or bubbles can be calculated as follows by inserting all the r- values in equation 3.

Parameters	Radius (R) (mm)	Number of bubbles (N)
R1	1.5	1910
R2	2	806
R3	2.5	413
R4	3	239
R5	3.5	150

Based on the above calculation, a total of fifteen models were developed.

The following are 3D CAD models developed based on Equation 3 above calculations at volume fractions of 5%, 10% and 15% of air voids in which the air bubbles are randomly dispersed or distributed in the aluminum foam boxes; this is for forming aluminum foam as shown in the figure below.



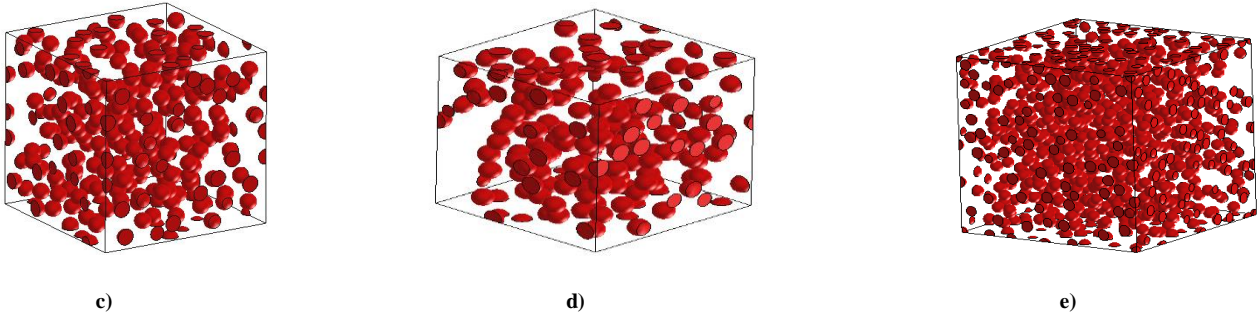


Fig. 4 Geometrical Representation of voids inside Al metal foam box at the radius of: a) 1.5 mm b) 2mm c) 2.5 mm d) 3 mm and e) 3.5 mm

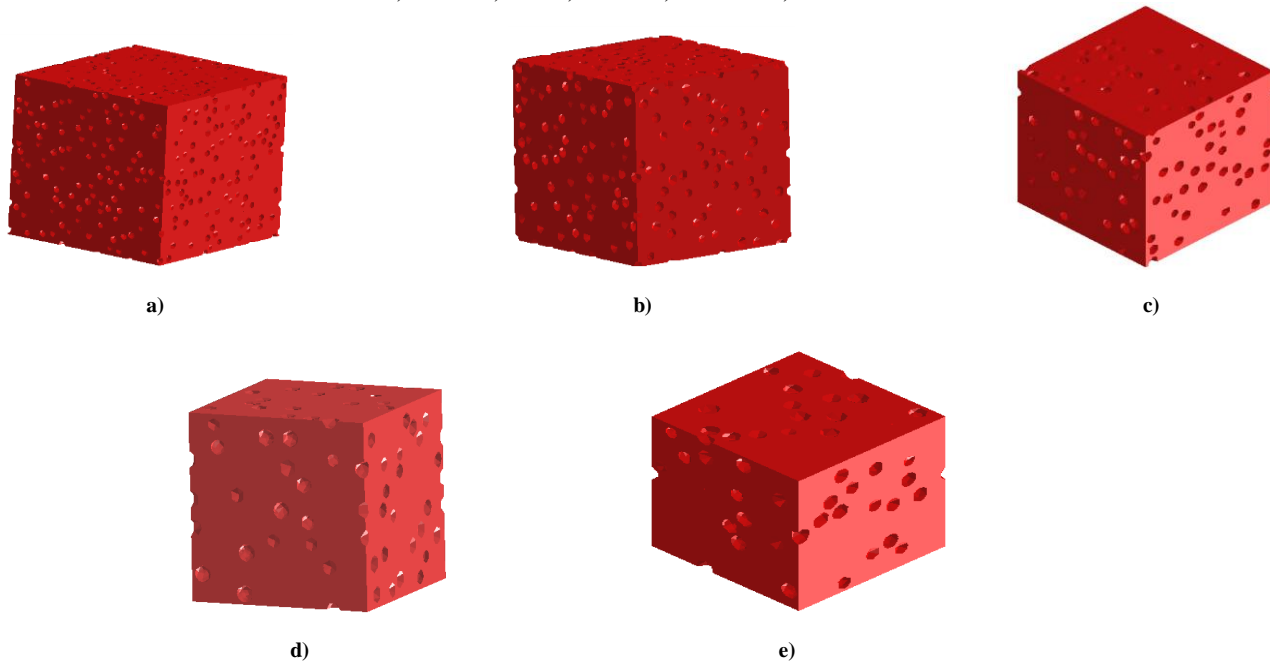


Fig. 5 Models Representation of RVE with 10% void, at the radius of: a) 1.5 mm b) 2mm c) 2.5 mm d) 3 mm and e) 3.5 mm

As shown in **Error! Reference source not found.** above, as the radius size increases from 1.5 mm to 3.5 mm, the number of bubbles decreases from 1910 to 150.

4.2. Boundary Conditions

The CAD model is also fully constrained at the right, and the steel plate is rigid and fixed support condition. This speed is used at the left rigid moving steel plate and on Al foam, as presented in Figure 6 above. The CAD model and the contact are assumed to be frictionless. The material data used all the while numerical evaluation on ANSYS workbench of aluminum foam is Explicit materials, aluminum 7075-T6 alloy for foam specimen and structural

steel for left and right plates. Johnson Cook plasticity model is used. The failure evaluation for this nonlinear aluminum foam is plastic strain failure with the maximum equivalent plastic strain of 0.75. For reduced speed impact simulation, 7 m/sec initial velocities are used.

The total mass of the impactor and the Aluminum foam is 12.0003923 kg for 5%, 12.003138 kg for 10% and 11.996352 kg for 15%. The same impactor square shape of dimension 46 mm X 46 mm is used for all models. The material model for the impactor has been chosen to be rigid, and the foam is crushable foam.

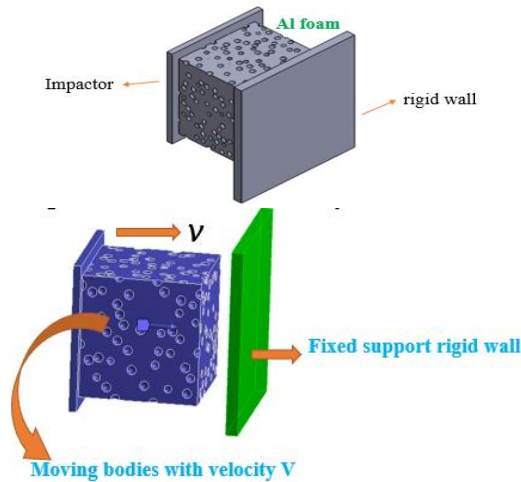


Fig. 6 Specimen for impact simulations

4.3. Cell Density Calculation

The cell density for this Al foam can be calculated as follows:

$$\text{Cell density } (C_D) = \frac{N}{V} \dots \dots \dots 4$$

Where: N-Number cell and V- Volume of Al foam cube
 This cell density calculation is used to know the distribution of the cells/bubbles on the entire Al foam model per volume. As expressed in the equation above, when the number cell decreases, the probability of distribution of the bubbles also decreases because of the volume of the Al foam constant. It is more clearly indicated in **Error! Reference source not found.** below.

Table 3. Cell density distribution for all models

Radius R (mm)		Cell Density (CD)
R1	1.5	0.7074
R2	2	0.298
R3	2.5	0.153
R4	3	0.0885
R5	3.5	0.05556

As a result, shown in **Error! Reference source not found.** and Table 3, the distribution of bubbles is highly dense for smaller radii and less dense for higher radii. **Error! Reference source not found.** shows the dense distribution of the bubbles with a smaller radius and the sparse distribution of bubbles with a higher radius. This is because the analyses are conducted on the same dimension (30mm x 30mm x 30mm) of the models. Look at the following diagrams for detail.

A.

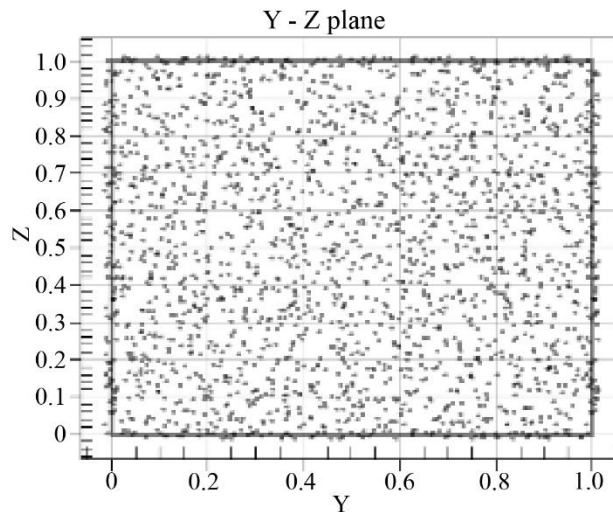
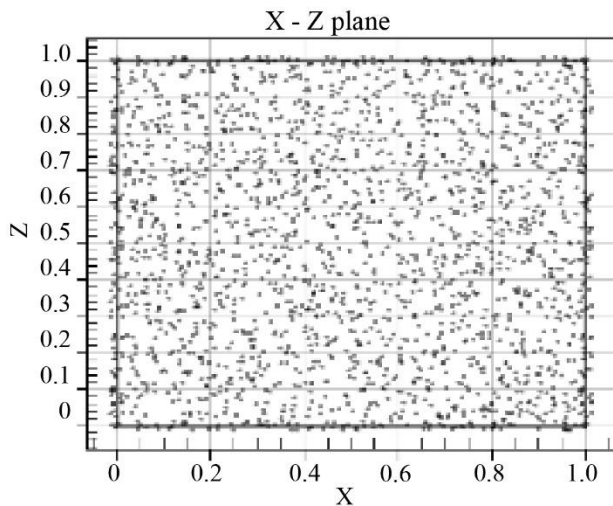
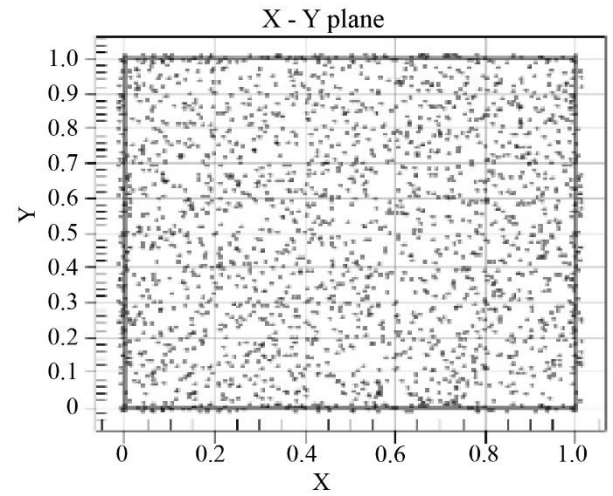


Fig. 7 Graphical representation of the position of voids distributions inside the Al metal foam specimen at the radius of 1.5 mm

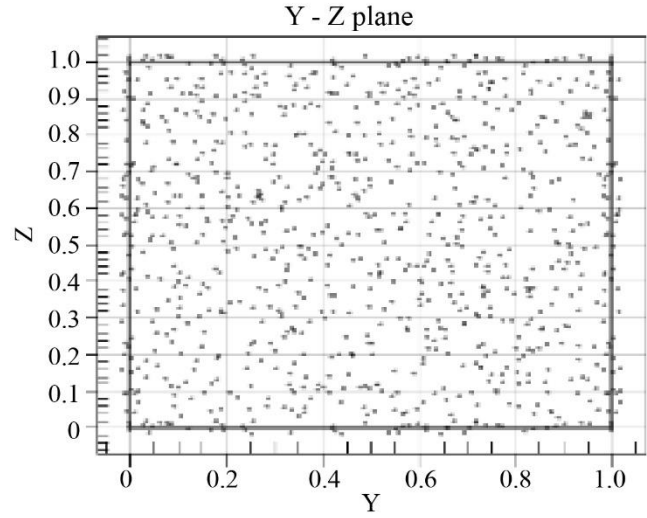
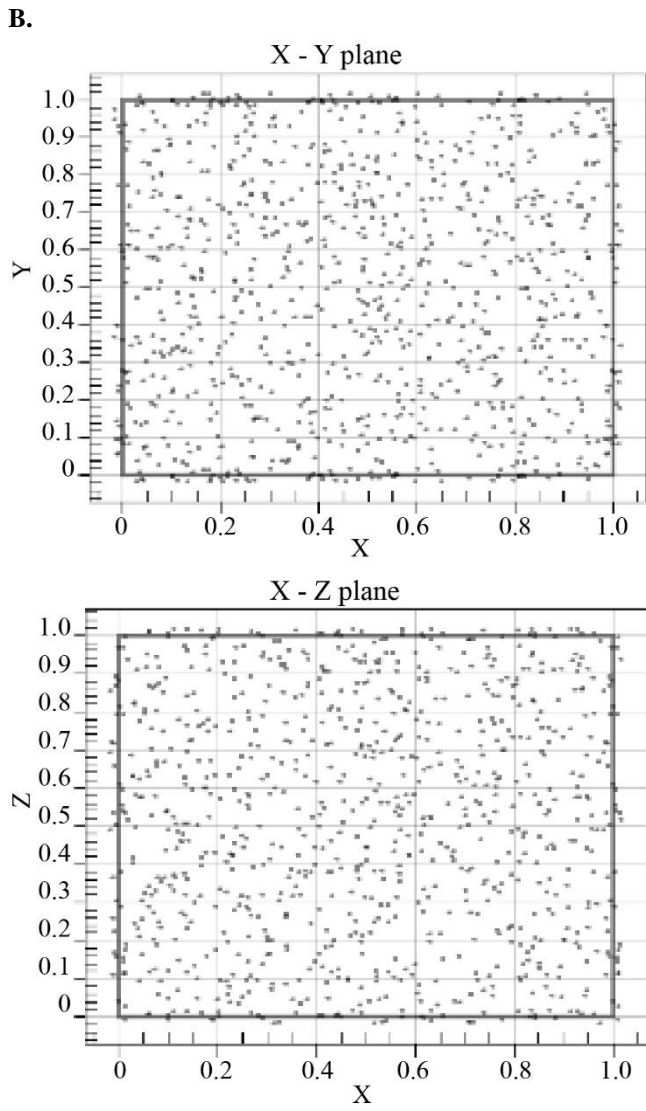
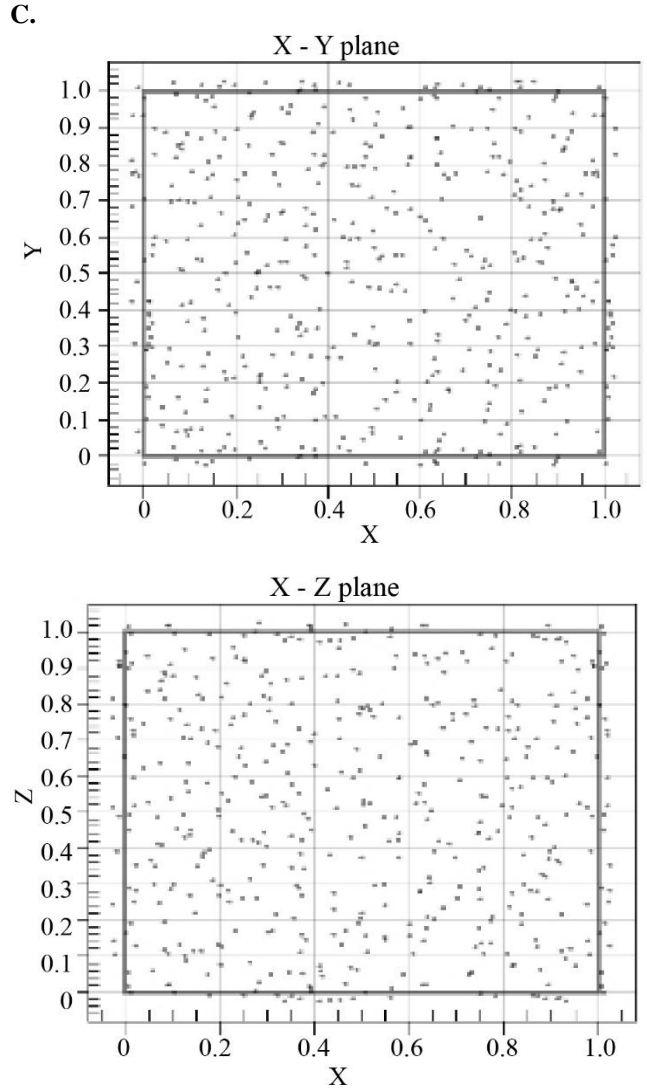


Fig. 8 Graphical representation of the position of voids distributions inside the Al metal foam specimen at the radius of 2mm



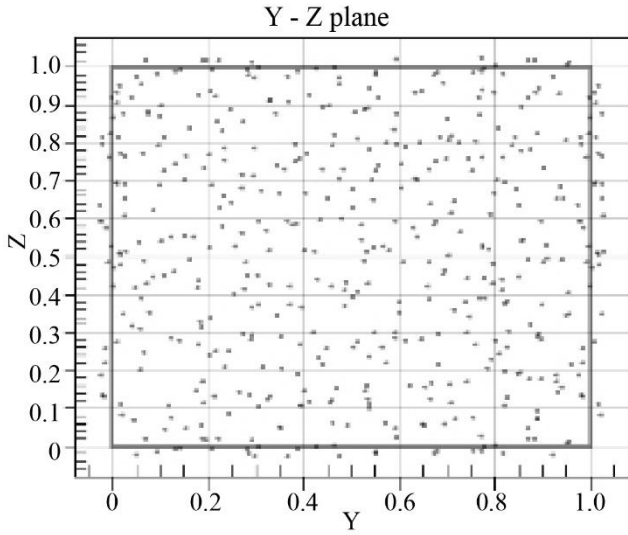


Fig. 9 Graphical representation of the position of voids distributions inside the Al metal foam specimen at the radius of 2.5 mm

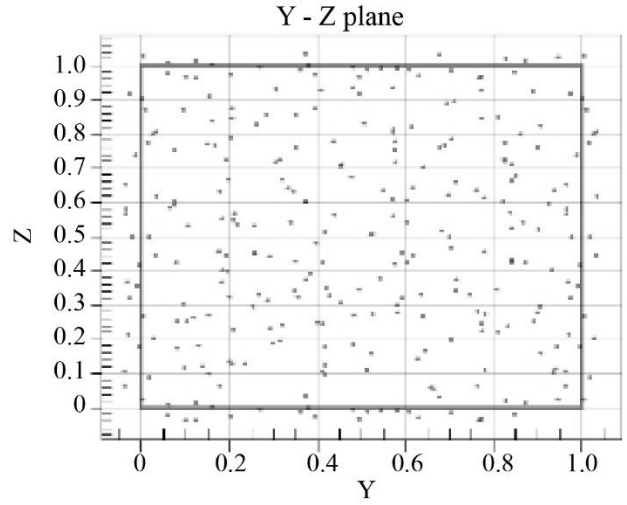
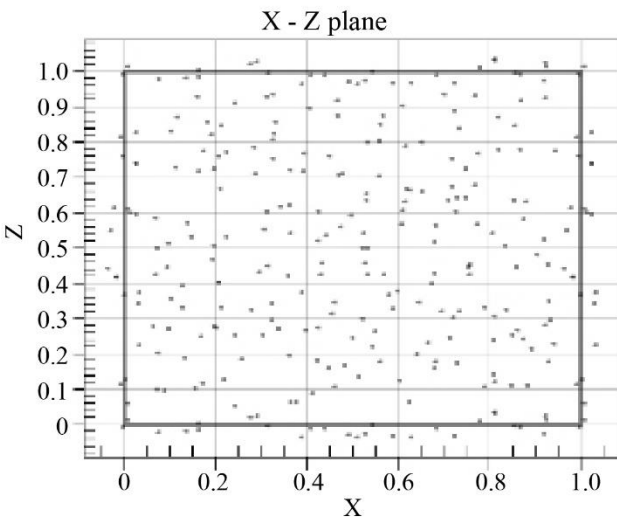
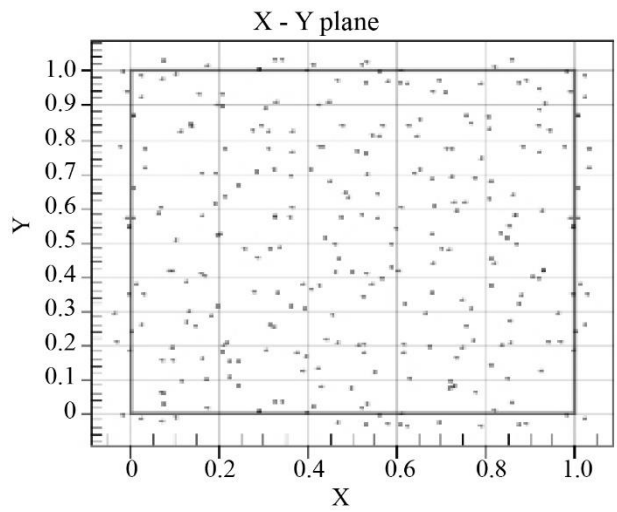
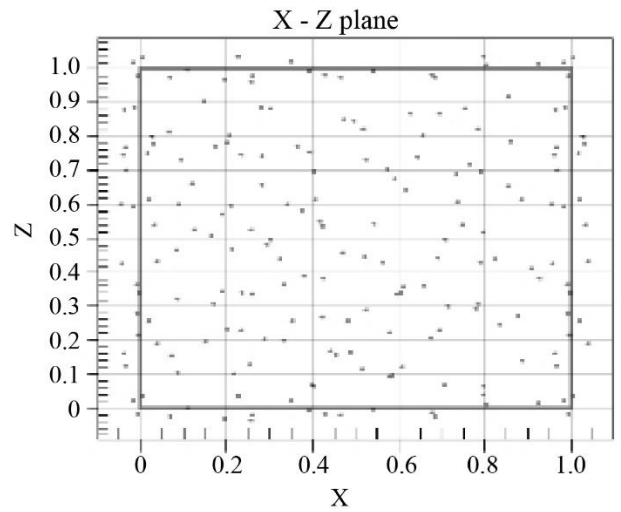
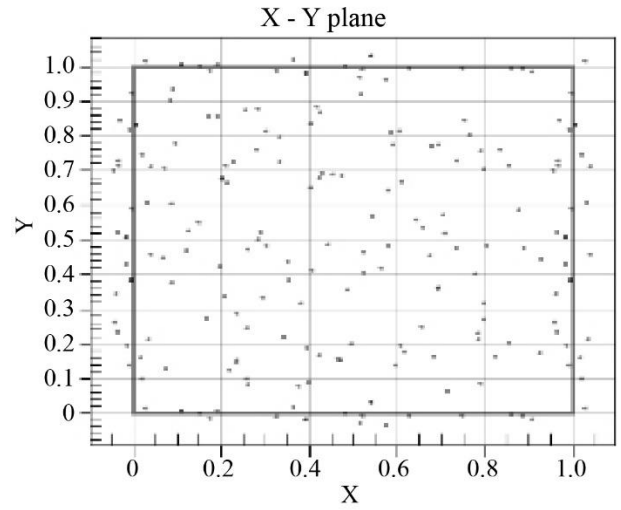


Fig. 10 Graphical representation of the position of voids distributions inside the Al metal foam specimen at the radius of 3 mm

D.



E.



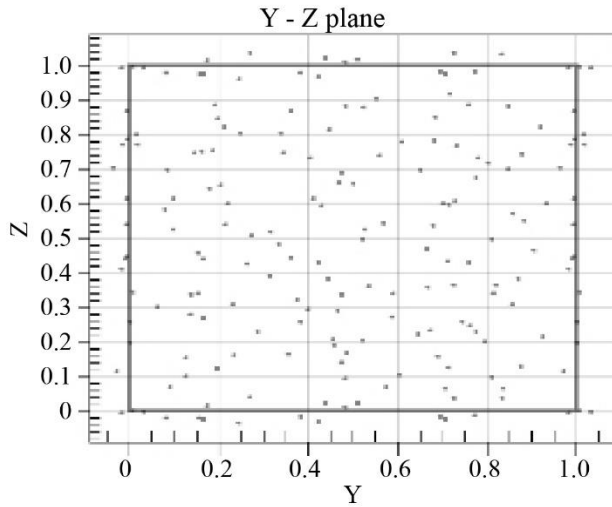


Fig. 11 Graphical representation of the position of voids distributions inside the Al metal foam specimen at a radius of 3.5 mm

The above diagram shows the random distribution of the voids in cubic elements in three different coordinates. The above distribution diagrams show that the distribution of air bubbles is randomly distributed throughout the entire foam element parts at R1, R2, R3, R4 and R5, respectively. Again, this diagram shows that the distribution of bubbles is densely populated at the minimum radius, and at a large radius, low bubbles appear. The distribution of the bubbles for all fifteen models at 5%, 10% and 15% void fractions are in the same fashion.

Percentages (%)	Void fraction	Density (kg/m ³)	Relative density
5	0.05	2664	0.951
10	0.1	2523.6	0.901
15	0.15	2383.4	0.851

4.4. Porosity

Porosity is known as the percentage of void spaces present in solid aluminum. Porosity plays a very important role as the density in deciding the foam quality. As the density of the foam decreases, the porosity increases. However, the increase in porosity not helps; instead, for the foam, uniform porosity is the important parameter. In the cast parts, porosity is a problem, but in this aluminum foam synthesis, the main objective is to develop uniform porosity. The simple concept of evaluating the % porosity, which is given by:

$$\% \text{ of Porosity} = \frac{\rho_{Al} - \rho_{AF}}{\rho_{Al}} \times 100 \dots \dots 5$$

In order to determine the porosity of the aluminum foam, the density of the foam is calculated by the volume and mass of the samples. Later, the foam specimen's porosity (p) is calculated using the following relation.

$$P = 1 - \frac{\rho_{AF}}{\rho_{Al}} \dots \dots \dots 6$$

Where ρ_{AF} – density of the Aluminum foam
 ρ_{Al} – density of the pure aluminum
 Or the porosity of the aluminum foam can be calculated from the equation

$$\text{Porosity \%} = (1 - \rho^*) \times 100 \dots \dots \dots 7$$

Where ρ^* - the relative density of aluminum foam.

5. Results and Discussion

The result from the analysis includes the energy absorption, effects of pore size, effects of Percentage composition, comparison of different foaming agents and weight reduction of Al foam.

5.1. Energy Absorption Analysis for Aluminum Foam

To assess the crashworthiness of the studied Al foam or compare the performance of different foam structures, it is necessary to establish proper criteria. These criteria must correlate the numerical results with the quality of the structures in several fields[19]. Energy absorption (EA) is used to evaluate the crashworthiness in determining the crashworthiness.

The specific energy absorbed (SEA) shows the capability of a structure to absorb the deformation energy. Specific energy absorption (SEA) is represented as the absorbed energy (EA) per structure mass[20]. In other words, it denotes the energy absorbed per unit mass of the absorber, which can be calculated as:

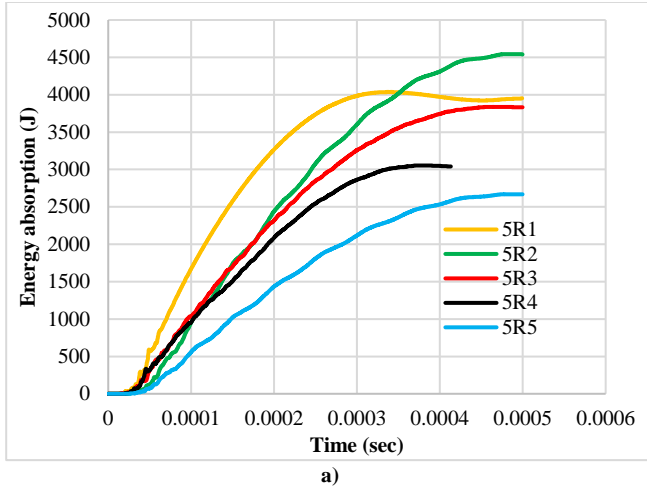
$$\text{SEA(J/kg)} = (\text{Energy (J)}) / \text{Mass of the moving structure} \dots \dots \dots 8$$

Where M – Total mass of the moving structure

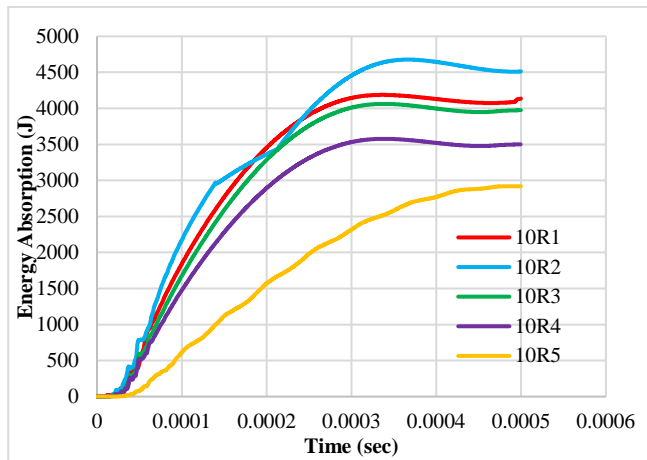
EA – Energy absorption during impact.

By rearranging equation (8) above from this formula, we can calculate total Energy absorption, which is given by:

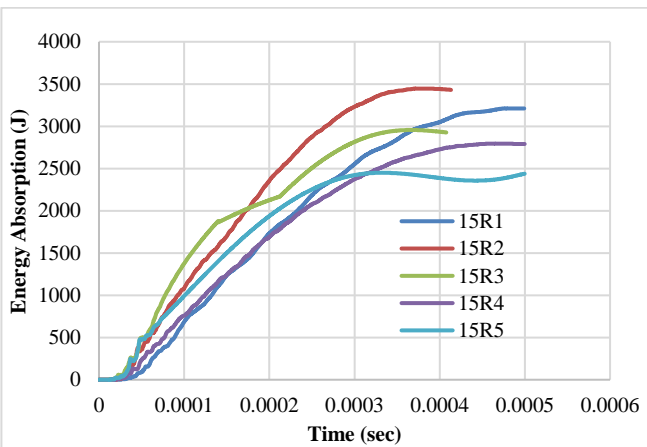
$$\text{EA(J)} = \text{SEA} \times \text{M} \dots \dots \dots 9$$



a)



b)



C)

Fig. 12 Energy Absorption comparison for models at 5%, 10% and 15%, respectively

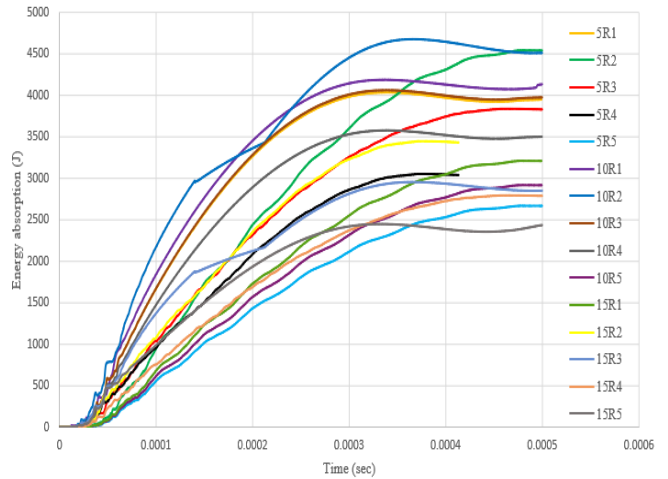


Fig. 13 Total overall Energy Absorption comparison for all models

Figure 13 compares the total overall energy absorption for all fifteen Al foam models. The energy absorption for the model with 10% composition is at the higher region with optimum deflection time compared with 5% and 15% models. This shows that the increase of percentage composition of air voids beyond 10% decreases the material's stiffness relatively compared to 10% air voids foamed Aluminum foam.

In the same manner in C)

Fig. 12 a, b and c, as porosity increases, the energy absorption decreases, except for models at 1.5mm.

C)

Fig. 12 and Fig. 13 show that the elastic properties decrease with increasing porosity and percentage composition of the Al foam. This decrease in results is because higher porosity elastic deformation may easily occur, resulting in a reduction in energy absorption rate. This leads to selecting the optimum air voids composition for the best energy absorption.

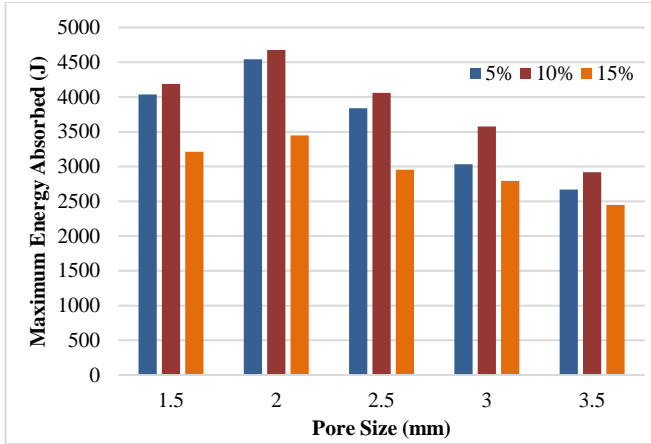


Fig. 14 The energy absorption vs model

5.2. The Effect of Percentage Composition on the Impact of Energy Absorption

Fig. 13 shows the model at 10% void fractions are maximum in energy absorption capacity compared to other models with 5% and 15% voids percentage. The characteristics of the material to absorb good impact energy for automotive applications should exhibit slow and progressive collapse bubbles (voids with air) and a smooth energy absorption graph. As in C)

Fig. 12 and Fig. 13, the percentage composition also highly affects the impact energy absorption rate of Al foam.

5.3. The Effect of Pore Size on the Impact of Energy Absorption

As shown in all the graphs above and Fig. 14 below, the increase of pores from 1.5 mm to 3.5 mm leads to a decrease in the stiffness characteristics of the Aluminum foam. This implies that low-stiffness material results in low-impact energy absorption.

As shown in Fig. 14 for the model, at 5%, 10%, and 15%, the energy absorption decreases when the bubble radius (pore size) increases from 1.5 mm to 3.5 mm. However, the models shown in Figure 14 give the parabolic shape, which means that it is minimum at starting for the minimum bubble radius and increases with an increase in radius up to 2mm, then decreases for a higher bubble radius. Therefore, these show the optimum bubble size with respective percentage composition of Aluminum foam for the best impact energy absorption applications is the model at 10% composition with 2mm pore size. Because herein this figure model with 10% at radius $R_2 = 2$ mm bubble size absorbs energy by 44.18% more than models at 5% and 53.41% more than models at 15% composition.

5.4. The Effect of a Foaming Agent on the Impact of Energy Absorption

In the process of foaming Aluminum foam for impact energy absorption applications in automotive and aerospace engineering, fine ceramic Silicon Carbide (SiC) and Boron Carbide (B_4C) foaming agents were used as additions to enhance the performance of Al foams. Results indicated that the additions of the ceramic particle, such as SiC, showed a moderate effect, whilst the B_4C showed a minor effect on the energy absorption enhancement of Al foam[16][21] [22].

However, now this research introduces another foaming agent called bubbles (void with air) for Aluminum foaming for impact energy absorption purposes.

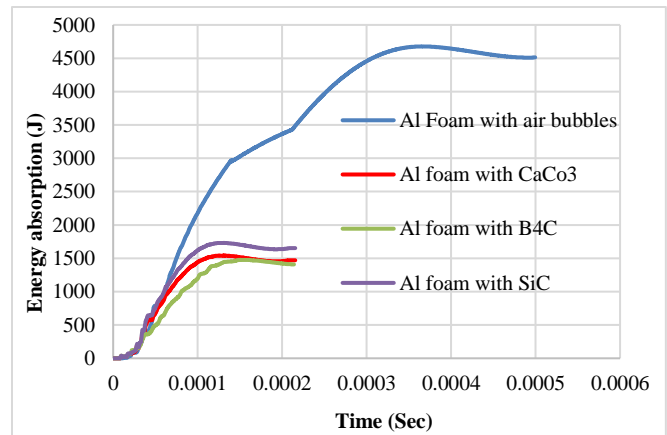


Fig. 15 Comparison of Al foaming agents for energy absorption

As shown in Fig. 15 above, the maximum energy absorbed by the models is 4676.937 J, 1653.84 J, 1540.2 J and 1476.69 J for Al foam with bubbles (voids with air), Al foam with SiC, Al foam with $CaCo_3$ and Al with B_4C respectively. As indicated in this figure, using bubbles (voids with air) for Al foaming enhances or increases the energy absorption capacity of the candidate materials from 1653.84 J, 1540.2 J and 1476.69 J to 4676.937 J than using SiC, $CaCo_3$, and B_4C respectively. In addition to these, when the new Al foam at 10% void fraction is compared to the other existing foaming agent called silicon carbide, its energy absorption was increased by 92.8% from 17.33 MJ/M³ to 242.77 MJ/M³ and 86.4% from 33MJ/M³ to 242.77 MJ/M³[6][21]. On the other hand, Fig. 15 shows that using air bubbles (voids with air) as a foaming agent makes the candidate material lighter in weight than other foaming agents. This intern uses for fuel economy for vehicles.

6. Conclusion

In the numerical analysis of closed-cell Aluminum foam for energy absorption purposes, specifically for vehicle frontal impact condition applications, the energy absorption capacity of Al foam should be kept high, and the weight of the foam material should be as low as possible for fuel

economy. Therefore, from the previous results and discussions, the closed-cell Aluminum foam model with a 10% void fraction at a bubble size radius of 2mm is selected as a new material to manufacture impact structures for automotive and aerospace engineering companies.

The following conclusions are drawn from this paper.

- The energy absorption capacity of closed cell Al foam at a pore size of 2 mm with 10% porosity percentage composition was 4676.937 J.
- To absorb 4676.937 J of impact energy during a collision, the candidate closed cell Al foam deforms a maximum of 1.4493 mm.
- The mass of the closed cell Aluminum foam with air bubbles was reduced by 7.3% from 0.14104 kg to 0.068138 kg and 6.8% from 0.13618 kg to 0.068138 kg than using CaCo₃ and B4C foaming agents, respectively. These obviously show that using air as a foaming agent makes the specimen lighter than other particles.

The energy absorption capacity of closed cell Al foam with bubbles (void with air) was increased by 74.77% from 1653.84 J to 4676.937 J, 76.5% from 1540.2 J to 4676.937 J and 77.4% from 1476.7 J to 4676.937 J than using SiC, CaCo₃ and B4C foaming agents respectively, and increased from 17.33 MJ/M³ to 242.77 MJ/M³ and from 33 MJ/M³ than using Silicon Carbide as a foaming agent and Aluminum foam filled steel. These results indicate that the foaming of closed cell Al metal with randomly and finely distributed pores (voids with air) increases the materials' stiffness to absorb more energy with optimum time.

Finally, the pore size, percentage composition and foaming agent (particles) highly affect the impact energy absorption of Al foam in addition to its microstructure arrangement.

Acknowledgment

The researcher would like to thank our almighty god for everything.

References

- [1] Xiaoqin Hao et al., "Factors Affecting the Compression and Energy Absorption Properties of Small-Sized Thin-Walled Metal Tubes," *International Journal of Aerospace Engineering*, vol. 2020, 2020. *Crossref*, <https://doi.org/10.1155/2020/6135925>
- [2] Gauri B. Mahajan, and Dinesh N. Kamble, "Crash And Impact Strength Analysis of Structural Component of the Vehicle for Occupant Safety," *International Journal of Scientific & Technology Research*, vol. 4, no. 12, pp. 4288–4293, 2015.
- [3] Ahmet Güner, Mustafa Merih Arıkan, and Mehmet Nebioglu, "New Approaches to Aluminum Integral Foam Production with Casting Methods," *Metals - Open Access Metallurgy Journal*, vol. 5, no. 3, pp. 1553–1565, 2015. *Crossref*, <https://doi.org/10.3390/met5031553>
- [4] Hadi Saputra, Jamasri, and Heru S. B. Rochardjo, "The Prediction of Energy-Absorption on the Car Crush Box," *3rd International Conference on Science and Technology - Computer (ICST)*, pp. 51–56, 2017. *Crossref*, <https://doi.org/10.1109/ICSTC.2017.8011851>
- [5] Kresimir Grilec, Gojko Maric, and Katica Milos, "Aluminium Foams in the Design of Transport Means," *Promet-Traffic & Transportation*, vol. 24, no. 4, pp. 295–304, 2012. *Crossref*, <https://doi.org/10.7307/ptt.v24i4.437>
- [6] Hamza A. Osman, "Characterization of Aluminium Foam Produced From Aluminium Scrap By Using CaCo₃ as Foaming Agent," *Journal of Engineering Science*, vol. 45, no. 4, pp. 448–459, 2017. *Crossref*, <https://doi.org/10.21608/JESAUN.2017.116283>
- [7] Ulhas K. Annigeri and G. B. Veeresh Kumar, "Effect of Reinforcement on Density, Hardness and Wear Behavior of Aluminum Metal Matrix Composites: A Review," *Materials Today Proceedings*, vol. 5, no. 5, pp. 11233–11237, 2018. *Crossref*, <https://doi.org/10.1016/j.matpr.2018.02.002>
- [8] Jiannan Sun et al., "A High-Similarity Modeling Method for Low-Porosity Porous Material and Its Application in Bearing Cage Self-Lubrication Simulation," *Materials (Basel)*, vol. 14, no. 18, pp. 5449, 2021. *Crossref*, <https://doi.org/10.3390/ma14185449>
- [9] M. Aboraia, R. Sharkawi, and M. A. Doheim, "Production of Aluminium Foam and the Effect of Calcium Carbonate as a Foaming Agent," *Journal of Engineering Sciences*, vol. 39, no. 2, pp. 441–451, 2011.
- [10] N. Gupta et al., "Testing of Foams," *Handbook of Mechanics of Materials*, pp. 2083 - 2122, 2019. *Crossref*, https://doi.org/10.1007/978-981-10-6884-3_50
- [11] H. K. Farahani, M. Ketabchi, and Sh. Zangeneh, "Determination of Johnson – Cook Plasticity Model Parameters for Inconel718," *Journal of Materials Engineering and Performance*, vol. 26, pp. 5284–5293, 2017. *Crossref*, <https://doi.org/10.1007/s11665-017-2990-2>
- [12] Vignesh Sampath, C. Lakshmana Rao, and Santhosh Reddy, "Energy Absorption of Foam Filled Aluminum Tubes Under Dynamic Bending," *Procedia Manufacturing*, vol. 7, pp. 225–233, 2017. *Crossref*, <https://doi.org/10.1016/j.promfg.2016.12.054>
- [13] X. C. Xia et al., "Effects of Porosity and Pore Size on the Compressive Properties of Closed-Cell Mg Alloy Foam," *Journal of Magnesium and Alloys*, vol. 1, no. 4, pp. 330–335, 2013. *Crossref*, <https://doi.org/10.1016/j.jma.2013.11.006>
- [14] Ana M. Amaro et al., "Mechanical Characterization of Different Aluminium Foams at High Strain Rates," *Materials*, vol. 12, no. 9, pp. 1428, 2019. *Crossref*, <https://doi.org/10.3390/ma12091428>
- [15] Nallely Trejo Rivera, Jesus Torres Torres, and Alfredo Flores Valdés, "A-242 Aluminium Alloy Foams Manufacture from the Recycling of Beverage Cans," *Metals (Basel)*, vol. 9, no. 1, p. 92, 2019. *Crossref*, <https://doi.org/10.3390/met9010092>

- [16] Ramasamy Karuppasamy, N. M. Sivaram, and Debabrata Barik, "Compressive Strength of Open Cell AL-SI 12 -FE Foam Produced Through Sand Casting Method," *International Journal of Mechanical Engineering and Technology*, vol. 9, no. 6, pp. 459–466, 2018.
- [17] R. Pippin, and C. Motz "Deformation Behaviour of Closed-Cell Aluminium foams in Tension," *Acta Materialia*, vol. 49, no.13, pp. 2463-2470, 2001. *Crossref*, [https://doi.org/10.1016/S1359-6454\(01\)00152-5](https://doi.org/10.1016/S1359-6454(01)00152-5)
- [18] Hamza Sulayman Abdullahi. Yicheng liang, and Shuming Gao, "Predicting The Elastic Properties of Closed-Cell Aluminum Foams : A Mesoscopic Geometric Modeling Approach," *SN Applied Science*, vol. 1, no. 380, 2019. *Crossref*, <https://doi.org/10.1007/s42452-019-0382-y>
- [19] Tiago Miguel and Encarnacao Nunes, "Multi-Objective Design Optimization of a Frontal Crash Energy Absorption System for a Road-Safe Vehicle," *Aerospace Engineering*, 2017.
- [20] N.A. Rahman et al., "Energy Absorption Capability and Deformation of Laminated Panels for Armoured Vehicle Materials," *International Journal of Automotive and Mechanical Engineering*, vol. 13, no. 3, pp. 3657–3668, 2016. *Crossref*, <https://doi.org/10.15282/ijame.13.3.2016.10.0300>
- [21] Dipen Kumar Rajak, L. A. Kumaraswamidhas, and S. Das, "Experimental Analysis to Improve Energy Absorption Properties of Rectangular Metal Section Subjected to Axial Loading," *Materials Today Proceeding*, vol. 3, no. 6, pp. 2207–2212, 2016. *Crossref*, <https://doi.org/10.1016/j.matpr.2016.04.127>
- [22] G. Kavei, "Mechanical Properties of Aluminum Foam Fabricated by Aluminum Powders with Na or Carbamide Replica," *AASCIT Journal of Materials*, vol. 1, no. 2, pp. 22–30, 2015.